JOINT EUROPEAN TORUS JET

JET–P(87)34

M. Cox and D.H.F. Start

Aspects of Combined ICRF and Neutral Beam Heating and Current Drive

Aspects of Combined ICRF and Neutral Beam Heating and Current Drive

M. Cox[1] and D.H.F. Start

JET-Joint Undertaking, Culham Science Centre, OX14 3DB, Abingdon, UK

[1]Culham Laboratory, Abingdon, Oxon, OX14 3DB, U.K.

Preprint of a paper to be submitted for publication in Proceedings of 1987
International Conference on Plasma Physics, Kiev, U.S.S.R., 6th April - 12th April 1987

ASPECTS OF COMBINED ICRF AND NEUTRAL BEAM HEATING AND CURRENT DRIVE

M Cox and D F H Start*

Culham Laboratory, Abingdon, Oxon, OX14 3DB, UK
(UKAEA/Euratom Fusion Association)

* JET Joint Undertaking, Abingdon, Oxon, OX14 3EA, UK

1. INTRODUCTION

Neutral beam (NB) and Ion Cyclotron Radio Frequency (ICRF) heating have individually been studied in great detail over a number of years both theoretically and experimentally. In addition several machines, both past and present, have used both methods simultaneously[1-3]. Results from these machines indicate that, in global terms, the two systems are compatible and no serious deleterious effects have yet been observed. In particular the heating efficiency of the combined scheme is similar to that observed for each of the schemes used independently. There are, however, indications that direct coupling of ICRF power to the beam ions can occur in some circumstances[4]. It is appropriate, therefore, to consider whether such coupling could lead to either beneficial or deleterious effects. In addition to this rather general motivation for studying combined neutral beam and ICRF heating there are a number of specific points which justify effort in this area.

Firstly, any interaction between the ICRF waves and the neutral beams will give rise to an additional damping of the wave power which, if large, could alter the profile of wave power deposition in the plasma. Furthermore the subdivision of collisional power transfer to background ions and electrons may be altered. Secondly, it has been suggested by previous work [5 - 7] that coupling of ICRF power to beam ions may produce an enhancement of the beam fast-ion (and hence the beam-driven) current. Thirdly, the increase in the number of particles above the beam injection velocity due to RF acceleration of injected beam ions will influence the fusion reactivity of the beam distribution and hence may offer means of enhancing the Q of the plasma. Finally, it should be noted that any ICRF heating and/or current-drive scheme which utilises a deuterium resonance is also prone to coupling power to the α-particle distribution in a burning plasma (since $\omega_c(D) = \omega_c(^4H_e)$) which in turn has the same characteristics as a beam distribution in a neutral beam heated plasma. If coupling to the α-particles does occur it could lead to a enhanced loss of fusion power since the increase in

the average perpendicular velocity which arises will increase the fraction of α-particles near the loss cone

Most of the potential effects of combined ICRF and NB heating outlined above have been considered in previous studies[5] [6] [7] using models of varying degrees of sophistication. The validity of the various simplifying assumptions that have been made in these studies can only be assessed if a comprehensive theoretical/computational model is available. The aim of the present paper is to summarise recent work at Culham Laboratory aimed at producing a model of both ICRF and combined ICRF and NB heating which includes all of the processes thought to be of importance. The diversity of effects of ICRF and NB heating used singly or combined and the large number of possible scenarios (ie minority ion or second harmonic heating for a wide variety of plasma species mixes) precludes an exhaustive exposition here. Instead the theoretical/computational model that has been developed will be summarised and then used to highlight a few aspects of heating and current-drive caused by combined heating. Results are presented as a function of minor radius in a JET-like plasma and for definiteness only fundamental heating of a hydrogen minority in a moderate density deuterium plasma will be considered.

The structure of the remainder of the paper is as follows: In Section 2 general aspects of the formulation of the problem are discussed and in Section 3 the model used to calculate the minority ion/beam distribution function is outlined. Section 4 then presents a selection of results and finally a summary is given in Section 5.

2. FORMULATION OF THE PROBLEM

The goal of any drive towards theoretical explanation of the physics of a wave heating scheme must be to include all physical effects which are deemed to be important in the experiments. This is actually very difficult for the following reason. The strength of the interaction between a particle of a given species and a wave depends on the form of the wave field along the orbit of the particle. This implies that the evolution of the distribution function of an ensemble of particles of that species also depends on the spatial variation of the wave field, $\underline{E}(\underline{r}, t)$. However, $\underline{E}(\underline{r}, t)$ is itself dependent on the strength of the wave absorption by the various plasma species which in turn is dependent on their distribution functions, $f_j(\underline{r}, \underline{v}, t)$. In order to obtain a fully self-consistent calculation of wave heating one would, therefore, ideally require a simultaneous solution for

$$f_j(\underline{r}, \underline{v}, t;\underline{E}) \text{ and } \underline{E}(\underline{r}, t; f_j)$$

where the subscript j is to be taken as including all species which interact with the wave

The simultaneous solution for these functions is extremely difficult and the general case is unlikely to be solved in the near future. In light of the difficulty of the general problem simplifying assumptions are clearly necessary. The most straight-foward approach is to treat the interdependence between $\underline{E}$ and f_j as a second order effect and to proceed with the calculation of $\underline{E}$ using model distributions (usually Maxwellians) for the plasma species. The wave field so derived can then be used to calculate the wave-particle interaction to be used in the solution for f_j. From these distribution functions another measure of the power deposition profile can then be obtained by integrating the wave operator over velocity space. If the deposition profile evaluated in this way differs significantly from that predicted by the wave propagation code then it is strictly speaking necessary to iterate the procedure (for example, by adjusting the temperature of the absorbing species in the wave code) until a self consistent solution is obtained. The first stage of such an iteration loop is already included in many ICRF wave calculations by using a temperature for the absorbing species which is higher than the background plasma temperature. All studies of ICRF heating have so far used models which decouple the calculation of $\underline{E}$ and f_j as just described. However not all the methods used are capable of ultimately producing self-consistent solutions by iteration. The two broad categories of approaches are as follows.

The first is to completely decouple the calculations of f_j and $\underline{E}$ by assuming a specific model form for the velocity space dependence of the wave operator and then to present the quantities of interest (eg the current driven or the fusion reactivity) as functions of the parameters of the model and the wave power absorbed. Application of such results to the experiments then relies on using independent wave propagation calculations to obtain the power absorbed and to infer 'reasonable' values for the parameters representing the velocity space dependence of the wave interaction. The major disadvantage of this approach is that it is difficult to extend the method to allow iteration of the procedure to obtain a self-consistent solution since the power absorbed is never independently calculated from the distribution function in terms of meaningful wave parameters. In addition the reliability of any results from such a method is heavily dependent on how closely the model form for the wave interaction approaches reality. It is known, for example, that predictions of ECRH current-drive efficiency derived using simple model forms can be considerable over-estimates compared with those obtained from more

realistic models of the wave interaction[8]. Nevertheless the method does have the advantage of simplicity and it is the one that has been adopted in all analytic and many computational calculations.

A second, more complicated, strategy is to determine the velocity space dependence of the wave interaction from a model of (or ultimately even the 'true') wave field within the plasma. The advantage of this approach is that the specific values of the parameters used in the model wave field can hopefully be chosen so that it contains all of the essential features of the wave field which exists in the experiment. This approach also has the advantage that it is conceptually quite straight-forward (although potentially time consuming) to derive an iteration scheme for obtaining a self-consistent solution since the wave power absorbed is independently calculated in each section of the cycle.

The work summarised in the present paper is based on the second approach using an extension of a model previously used for ECRH calculations[8]. Iteration to obtain self consistent solutions has not yet been performed. The wave and Fokker-Planck models used are summarised in the next section.

3. THE BOUNCE-AVERAGED FOKKER-PLANCK EQUATION

The Fokker-Planck equation for the ion distribution of the beam species on a given flux surface during combined ICRF and NB heating can be written symbollically

$$\frac{\partial f}{\partial t} = \left\langle \left(\frac{\partial f}{\partial t}\right)_c \right\rangle + \left\langle \left(\frac{\partial f}{\partial t}\right)_w \right\rangle + S(\underline{v}) - L(\underline{v}) \qquad (1)$$

where the terms on the right-hand side are, respectively, due to collisions, velocity space diffusion arising from the wave interaction, a particle source representing beam injection and a particle loss term. In this paper attention will be restricted to equilibrium solutions of eq.(1) (ie the left-hand side is set to zero). The implications of this on the balance between $S(\underline{v})$ and $L(\underline{v})$ will be discussed in Section 3.1. In eq.(1) the angular brackets denote an average over the particle orbit

$$\langle A \rangle = \left(\int \frac{d\chi}{v_\parallel}\right)^{-1} \int A \, \frac{d\chi}{v_\parallel} \qquad (2)$$

where χ is the poloidal angle and $v_\parallel$ is the velocity of the particle

parallel to the magnetic field line. As is usual it will be assumed that the width of the ion drift orbit is small so that an integral over the particle orbit is equivalent to an integral within the flux surface. This approximation is a good one for ions near thermal velocities but may be questionable for ions at high energies even in large tokamaks; inclusion of finite drift-orbit width is a difficult problem which will not be addressed here.

3.1 The Particle Source and Sink

In order to represent the injection of beam ions it is necessary to include a source of particles in the Fokker-Planck model. In reality the fast-ions deposited on a given flux-surface from the beam will be created over a large poloidal extent. The motion of ions around their orbit is, however, rapid compared with any of the collisional time-scales and it is therefore irrelevant at which poloidal angle, χ, any particular ion is created. All that is necessary is to transform the local value of $\eta = v_\parallel(\chi)/v$ to an invariant one. The particular choice made is the value of η on the outboard side of the flux surface, $\eta_0 = v_\parallel(\chi = 0)/v$. The speed of the ion, v, is of course already an invariant on this time-scale. The particular form for $S(v, \eta_0)$ used here is a narrow gaussian centred around η_{inj}.

Equilibrium solutions of eq.(1) are only possible if the rate of particle creation from $S(v, \eta_0)$ is exactly balanced by an equal loss of particles via $L(v, \eta_0)$. In reality the form of L will be determined by plasma transport processes which as yet cannot easily be modelled. However, provided that the loss of particles does not occur too close to the injection speed, the precise form of L does not influence the results significantly. For the purpose of this paper the loss will be taken to have a gaussian shape identical to a Maxwellian at the background ion temperature.

3.2 The Collision Operator

The collision operator for test particles of species j with a distribution of particles of species i is obtained from the expression

$$\left(\frac{\partial f_j}{\partial t}\right)_c = \frac{e^4 \ln\lambda}{4\pi\ \varepsilon_0^2\ m_j^2} \sum_i \nabla\cdot \left\{-f_j\ \nabla h_i + \frac{1}{2}\ \nabla\cdot(f_j \nabla\nabla g_i)\right\} \qquad (3)$$

Here h and g are the Rosenbluth potentials[9] and the sum i is over all plasma species. Note that the collision operator for self-collisions (ie, collisions between particles of the same species, i = j) is

non-linear in f_j since h_i and g_i involve integrations over f_j. In the present paper this non-linearity will be removed by assuming a Maxwellian distribution for the minority ion field particle distribution. This is a good approximation for minority ion ICRF heating since the density of the minority ions is necessarily small and self collisions are therefore a weak effect compared with collisions with the other plasma species. This is true even at high velocities since collisions with electrons are almost independent of velocity and are always strong compared with the self collision terms. The code which is described later does, however, have the capability of including the effect of self collisions by means of an iteration scheme using the full collision package of Kerbel and McCoy[11].

The specific form of the collision operator for collisions with Maxwellian background species averaged over a flux surface ('bounce averaged') is set out in detail elsewhere[10 11]. Here we simply note that the collision operator can be expressed as the divergence of a flux in velocity space in terms of the speed of the particle normalised to the background ion thermal speed, x, and the value of $v_\parallel/v$ of the particle at the outermost point on the flux-surface, η_0

$$\langle\left(\frac{\partial f}{\partial t}\right)_c\rangle = v_0 \sum_i \left[\frac{1}{x^2}\frac{\partial}{\partial x}(P_i) + \frac{1}{r}\frac{\partial}{\partial \eta_0}(Q_i)\right] \qquad (4)$$

where $r = |\eta_0| \int^{\eta} \frac{d\chi}{\eta}$ and the fluxes P_i and Q_i are functions of f_i, $\partial f_i/\partial x$ and $\partial f_i/\partial \eta_0$. We refer to refs. 10 and 11 for the precise form of P_i and Q_i.

3.3 The RF Diffusion Operator

As was described in Section 2, the RF diffusion operator used in the present study is derived from a model form of the wave intensity in the plasma rather than simply being a model form in velocity space coordinates directly. The wave operator appropriate to toroidal geometry, which was discussed in detail in ref.8, is

$$\langle\left(\frac{\partial f}{\partial t}\right)_w\rangle = \frac{1}{2}\frac{\partial}{\partial J_i}\left(\langle D_{ij}\rangle \frac{\partial f}{\partial J_j}\right) \qquad (5)$$

where $D_{ij} = [\Delta J_i \Delta J_j/\Delta t]$, J_i and J_j are constants of the unperturbed motion and the brackets in the expression for D_{ij} denote an average over the cyclic variables which are canonically conjugate to J_i and J_j. The constants of the unperturbed motion used are $\mu = v_\perp^2/2B$ and $J = \int v_\parallel d\chi$. It was shown in ref.8 that if the poloidal extent of the

resonant interaction is small then the components D_{ij} of the wave induced diffusion can be related to the single quantity

$$D_0 = <[(\Delta v_\perp)^2]>/2\Delta t \qquad (6)$$

where $<[(\Delta v_\perp)^2]>$ is the average of the square of the increment in perpendicular velocity arising from the wave heating which depends on, amongst other things, the form assumed for the RF wave field. The particular form used here to model ICRF heating of beam ions, and the analysis used in the evaluation of $<[(\Delta v_\perp)^2]>$, are extensions of those used by O'Brien et al [8] for modelling ECRH experiments to which we refer for details. Here we present only a summary of the model and the extensions that have been made to it.

Briefly, the model assumes that the wave is spatially localised in a 'beam' propagating at angle $\sin^{-1}\beta$ from perpendicular (such that its spectrum in $k_\parallel$ is centred on $k_{\parallel 0}$) with a gaussian power profile transverse to the beam and a model profile along the beam; the parameters used are derived from, respectively, full wave modelling of the antenna pattern and ray tracing calculations. Analytic approximations to D_0 are then obtained in various limits and from these the form of the wave interaction is constructed. This model has been changed in several ways:

(i) Elliptical rather than circular 'beam' cross-sections are included to allow closer matching to the 'beam' shapes predicted by full wave calculations[12].

(ii) The model form for the variation of wave power within the plasma has been replaced by a direct interpolation of the output from ICRF ray tracing or full wave codes.

(iii) The full Bessel function variation in $v_\perp$ has been retained (rather than the small argument expansions) since $k_\perp v_\perp/\Omega$ is not always a small quantity for ICRF parameters

(iv) The 'heating out of resonance' limit to the diffusion imposed by O'Brien et al has been omitted since relativistic effects are negligible for ions.

The expression for D_0 can then be written

$$D_0 = \frac{\pi}{16\tau}\left(\frac{e}{m}\right)^2 \left\{|E_+^0(R)|^2\, e^{-2y^2/H^2}\, J^2_{\ell-1}\left(\frac{k_\perp v_\perp}{\Omega}\right)\frac{1}{Wv_\parallel{}^3}\right\}\chi_{res}\,\frac{K}{\int d\chi/v_\parallel} \qquad (7)$$

where H is the scale height of the gaussian beam, χ_{res} is the poloidal angle at which the particle satisfies the resonance condition

$$\{\omega - \ell\,\Omega\,(\chi) - k_{\parallel} v_{\parallel}(\chi)\}_{\chi_{res}} = 0 \qquad (8)$$

and

$$K = \int \exp\left\{\frac{-\beta^2}{2L^2W^2}\left(\frac{\omega - \ell\Omega}{v_{\parallel}} - k_{\parallel}\right)^2\right\} d\chi. \qquad (9)$$

Here

$$W^2 = \frac{\beta^4}{L^4} + \left(\frac{\ell\Omega_T'}{2v_{\parallel}}\right)^2 \qquad (10)$$

and

$$\ell\Omega_T' = \frac{d\Omega}{dz}\left\{1 - \frac{(\omega - \ell\Omega)(1+\varepsilon)v_{\perp 0}^2}{2\,\ell\,\Omega_0(1+\varepsilon\cos\chi)\,v_{\parallel}^2}\right\} \qquad (11)$$

where all parameters are as defined elsewhere[8]

The most important feature of the above expression is that the extent of the wave diffusion in $v_{\parallel}$ is a function of W^2 which depends both on the width, L, of the beam in configuration space and a combination, Ω_T', of the variation of the cyclotron frequency and the parallel velocity of the particle as a function of distance along its orbit, z. In evaluating D_0 from K we make use of the same approximations as O'Brien et al[8] with the exception that D_0 is also required not to exceed the value appropriate to those particles which are near to 'tangent resonance [7 11]. (A particle is said to be at tangent resonance if it simultaneously satisfies $\nu = \ell\Omega_0 - \omega + k_{\parallel} v_{\parallel} = 0$ and $\dot{\nu} = 0$.) The latter limit applies to those trapped particles whose 'banana tips' (ie the point at which $v_{\parallel} \to 0$) are close to the resonance layer. This addition is necessary to avoid the non-physical $v_{\parallel}^{-3}$ singularity inherent in the expression for K which arises from a breakdown of an approximation in the analysis[8]. It is unnecessary to introduce the limiting form for tangent resonant particles in the case of ECRH since those electrons to which it applies are also subject to the much stronger effect of 'heating out of resonance'[8].

Examples of the velocity dependence of D_0 derived from the above model are shown in Figs.1(a)-(c) for the flux surfaces labelled (a)-(c)

in Fig.2. Each contour corresponds to a factor of two change in the amplitude of the wave diffusion coefficient (with D_0 increasing with increasing contour label). The wave parameters have been set to $k_{\|0} = 4m^{-1}$, the beam width L = 1.0m and the beam height H = 0.75m to match the predictions of a full wave ICRF code. Figure 2 also shows the form of $|E_+(R)|^2$ used and the position of the cyclotron resonance for ions having zero parallel velocity. From Fig.1 is is clear that D_0 is a complicated function, is widely spread in velocity space and changes considerably from one flux surface to another. Fig.1(c) also demonstrates that trapped particles are strong absorbers of wave power on flux surfaces which intersect the resonance layer. Furthermore it should be noted that the form of D_0 never approaches the ideal localised forms which are usually assumed in simple analyses.

4 NUMERICAL SOLUTION AND RESULTS

4.1 Numerical Solution

When discretised the above equations yield a conventional 9-point numerical scheme in the absence of particle trapping. When trapping is taken into account additional internal constraints have to be imposed on the distribution function at the boundary between trapped and passing particles so that conservation of the particle flux across it is ensured[8]. This leads to a 12-point operator in this region of velocity space. The implicitly differenced discretised equations, which have the same form as those described in Ref.10, are solved by using a direct gaussian elimination package (MA32) from the Harwell Subroutine Libary which uses a method that requires little memory and is optimised for the CRAY computer. For most cases a mesh size of roughly 150 points in speed and 50 in pitch-angle is adequate although meshes of up to $\sim$ 300 x 100 can be used when necessary. As mentioned earlier, only equilibrium solutions will be considered here; the code does enable the time evolution to be studied although only relatively few, large time-steps can be followed due to the rather lengthy full matrix solution which is needed at each step. However the method does have the advantage of numerical robustness and allows the solutions for the steady-state to be obtained in one step.

The boundary conditions that have to be imposed on the solution are the same as those used in the ECRH code BANDIT except that, in order to separate out the effect of ICRF heating of the ions arising from the beam from that due to heating of 'thermal' ions, we adopt a slightly different boundary condition at v = 0 as will now be described.

Figure 3A shows schematically the form of the ion distribution function for ICRF heating of 'thermal' and 'beam' distributions as, respectively, the bottom and top curves of the three shown. When quoting the additional effect of beams on any quantities of interest one would naively separate out the contribution arising from the two areas labelled (b) and (c) in Fig.3A since this is the total change resulting from combined NB and ICRF. However, this is not particularly useful in practice for the following reason: The increase in the value of the distribution function at v = 0 in the plasma due to the effect of the additional particles from the beam source cannot be predicted a priori since the particle confinement properties of the plasma are not well known. It follows from the linearity of the Fokker-Planck equation that the distribution calculated is actually uncertain to within a multiple of curve (a) in Fig.3A. Thus even if a particular ad hoc assumption is made for f(v = 0) the calculated quantities will effectively contain a contribution from the increase in the density of 'thermal' particles. In order to eliminate this coupling the following procedure is adopted.

If one defines

$$f(v,\eta_0) = f_1(v,\eta_0) + f_2(v,\eta_0) \tag{12}$$

the linearity of the Fokker-Planck equation used allows the following decomposition to be performed.

$$\left\langle\left(\frac{\partial f_1}{\partial t}\right)\right\rangle = \left\langle\left(\frac{\partial f_1}{\partial t}\right)_C\right\rangle + \left\langle\left(\frac{\partial f_1}{\partial t}\right)_W\right\rangle \tag{13a}$$

$$f_1(v = 0) = F \tag{13b}$$

$$\left\langle\left(\frac{\partial f_2}{\partial t}\right)\right\rangle = \left\langle\left(\frac{\partial f_2}{\partial t}\right)_C\right\rangle + \left\langle\left(\frac{\partial f_2}{\partial t}\right)_W\right\rangle + S - L \tag{14a}$$

$$f_2(v = 0) = 0 \tag{14b}$$

This allows the part of the distribution function, f_1, which is linear in f(v = 0) to be isolated from the distribution function, f_2, which is linear in the magnitude of the beam source. Linear combinations of f_1 and f_2 can then be used to construct the distribution function for any given minority ion density and beam power. This mathematical approach can also be justified on more direct grounds by noting that any change in, say, the power absorbed that arises solely from any increase in f(v = 0) (ie the incremented part of

the distribution function labelled (b) in Fig.3A) could have been obtained experimentally simply by increasing the minority ion density in the plasma (for instance by increasing the rate of gas feed) without the addition of any neutral beam power. Only the incremental distribution labelled (c) in Fig.3A (and shown separately in Fig. 3B) is a direct consequence of neutral beam injection.

4.2 Numerical Results

The calculations presented in this section were performed for a deuterium plasma (n_e = 2.5 x 10^{19} m^{-3}, T_e=T_i= 3keV) containing a 5% minority hydrogen component. The efficiencies of current-drive for two particular cases of combined ICRH and neutral beam heating are shown in Figs.4a and 4b as a function of ε = r/R for the resonance position indicated in Fig.2 (ie. resonance to the inside of the magnetic axis and tangent to a flux surface with ε = 0.034). The first case corresponds to beam injection parallel to the field (η_{INJ} = 1.0) and the second is representative of the injection angle in JET (η_{INJ} = 0.5). The efficiency quoted for the combined scheme is the incremented efficiency ie, the ratio of the change in the fast-ion current, ΔJ, resulting from the absorption of wave power P_{QL} (with all quantities in the normalised units of Cordey et al[13]). Also shown in Figs.4a and 4b are the efficiencies of current-drive using beams alone for the two injection angles. Notice that the efficiency of the combined wave and beam scheme is substantially lower than the beam efficiency in both cases. The efficiency is highest on flux surfaces near the magnetic axis which do not intersect the resonance (ie, ε < 0.034). This arises because the wave then interacts preferentially with ions having parallel phase velocities near optimum for current-drive. However, even on these flux surfaces the incremented efficiency of the combined scheme is lower by factors of ~ 2 and ~ 3 for, respectively, η_{INJ} = 0.5 and 1.0. The rapid fall of efficiency with increasing ε is due to a combination of four effects:

(i) increased absorption on lower velocity ions.
(ii) absorption by trapped particles (which carry no current).
(iii) absorption of power by ions with both positive and negative $v_\parallel$.
(iv) enhanced trapping of ions arising from increases in $v_\perp$ due to wave heating.

For beam injection at η_{INJ} = 0.5 the combined effects of (iii) and (iv) lead to a net reduction in the fast-ion current (ie, ΔJ < 0). This is also a feature of the current-drive efficiency obtained using ICRF alone with an asymmetric wave spectrum as shown in Fig.5.

The wave schemes are even less attractive for 'bulk' current-drive than the beam schemes but the large gradient in $\Delta J/P_{QL}$ does offer the prospect of making localised changes to the current-density profile eg, to modify the MHD behaviour of the plasma. The pure wave scheme is favoured in this application because it has somewhat higher efficiency than the combined scheme (at least for the parameters considered here) and, more importantly, it is considerably more flexible since the lack of a preferred toroidal direction (ie, the beam injection direction) implies that J can be driven with equal ease in either direction. An experiment using travelling ICRH waves with the resonance placed tangent to the q = 1 surface inboard of the magnetic axis is clearly of interest. Initial estimates indicate that the current density profile could be flattened over a radial extent of $\sim$ 0.1m at q = 1 surface in JET for $n_e = 2.5 \times 10^{19} m^{-3}$, T_e = 6keV, P_{QL} = 10MW with a wave directivity of 25%.

This latter point raises the question, where is the wave power deposited and is the deposition predicted by the Fokker-Planck code consistent with that obtained from ray tracing or a full wave code? The power absorption profiles derived from the Fokker-Planck code assuming the wave field given by the ray-tracing and full wave codes are shown in Fig.6 for the two combined and the 'pure' wave schemes. Also shown by the numerals 1 and 7 are the power absorption profiles that would be obtained if the distribution function was Maxwellian at, respectively, 1 and 7 times the background ion temperature. (The value of 7 T_i was chosen because this was used to calculate the absorption in the ray tracing code.) Note that the wave absorption profile is relatively insensitive to the scheme used and that the only significant area of discrepancy occurs for $\varepsilon < 0.05$.

The behaviour at small radii ($\varepsilon < 0.02$), where the absorption is on high $v_\parallel$ ions, is easily understood since the presence of a beam increases the number of ions which have sufficiently high $v_\parallel$ to resonate with the wave. In the pure wave scheme the parallel distribution is not significantly distorted and the absorption is only slightly higher than for a Maxwellian at the background temperature. The behaviour on flux surface near $\varepsilon \sim 0.04$ where the absorption decreases with increasing temperature for a Maxwellian distribution and is lowest for the beam schemes indicates, as expected, that the absorption is mainly on ions at low velocities. The relatively low values of power absorption compared with those for Maxwellian distribution suggest that quasilinear flattening is important in these cases.

Overall it seems that the power deposition profile predicted in the ray tracing code, which assumes the absorbing species is Maxwellian at 7 T_i, is a reasonable first approximation but that it may somewhat overestimate the power absorbed on flux surfaces which are inside or just cross the resonance layer. The broad conclusions of this paper are, therefore, not significantly affected by the lack of self consistency of the wave field calculation but the effect is sufficient to warrant further examination if detailed predictions of profile specific effects are needed.

5. CONCLUSIONS

We have studied a specific example of combined ICRF wave plus beam heating and current-drive in which the resonance is to the inside of the magnetic axis and the beam is used as a minority species. Even in the central regions of the plasma the current-drive efficiency of the combined scheme is lower than for the beams by a factor $\sim$ 2-3. Furthermore, the rapid decline in efficiency with minor radius leads to very much lower overall efficiency and the conclusion that combined schemes are of little interest for bulk current-drive. However the steep decline (and even reversal) in current-drive with radius allows the possibility of using the scheme to flatten the current density profile. Initial estimate suggest that $\sim$ 10-20MW of ICRF power could flatten the profile at the q = 1 surface on JET.

As in previous calculations of ICRF heating and current-drive, the results presented here do not calculate the wave field in a self-consistent manner since no allowance is made for changes in polarisation or absorption due to the presence of non-Maxwellian distributions. Initial results presented here suggest that the inclusion of a self-consistent wave field would not cause qualitative changes to the predictions. However if detailed calculations of profile specific quantities are required then further consideration of this effect is warranted.

ACKNOWLEDGEMENT

We would like to thank Dr V P Bhatnagar for providing the ICRF wave field profiles used in this paper.

REFERENCES

[1] Lallia P P et al., Invited Paper at 13th European Conf. on Plasma Physics., Published in Plasma Phys. and Cont, Fus. 28 (1986) 1211.

[2] Wagner F et al., Ibid p1225.

[3] Nagami et al, 11th Int. Conf. on Plasma Physics, and Cont. Nuclear Fus. Research, Kyoto, Japan, 1986. Paper IAEA-CN-47/A-II-2.

[4] Cottrell G A et al., Proc. of 7th APS Conf. on Applications of Radiofrequency Power to Plasmas, Kissimee 1987 to be pub. Also Abe T et al., Proc. of 14th European Conf. on Contr. Fusion and Plasma Physics, Madrid, 1987, to be published.

[5] Okano K, Inoue N and Uchida T., Nucl. Fusion 23(1983)235.

[6] Cox M and Start D F H., Nucl. Fusion 24(1984)399.

[7] Cox M et al., 12th European Conference on Controlled Fusion and Plasma Physics, Budapest 1985, Vol.II p.140.

[8] O'Brien M R, Cox M and Start D F H., Nucl. Fusion 26 (1986)1625.

[9] Rosenbluth M N, MacDonald R M and Judd D L., Phys. Rev. 107(1957)1.

[10] O'Brien M R, Cox M and Start D F H., Comp. Phys. Comms. 40(1986)123.

[11] Killeen J et al., "Computational Methods for Kinetic Models of Magnetically Confined Plasmas", published by Springer-Verlag, 1986.

[12] Bhatnager V P and Koch R., Nucl. Fusion 26 (1986)61.

[13] Cordey J G, Edlington T and Start D F H., Plasma Phys. 24(1982)73.

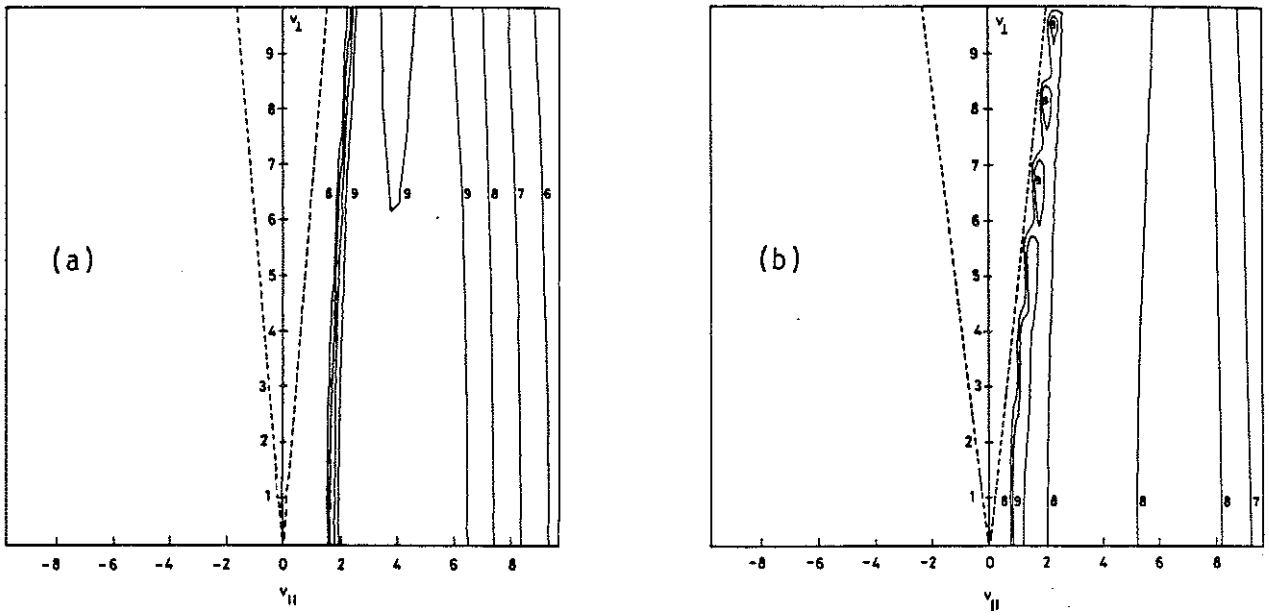

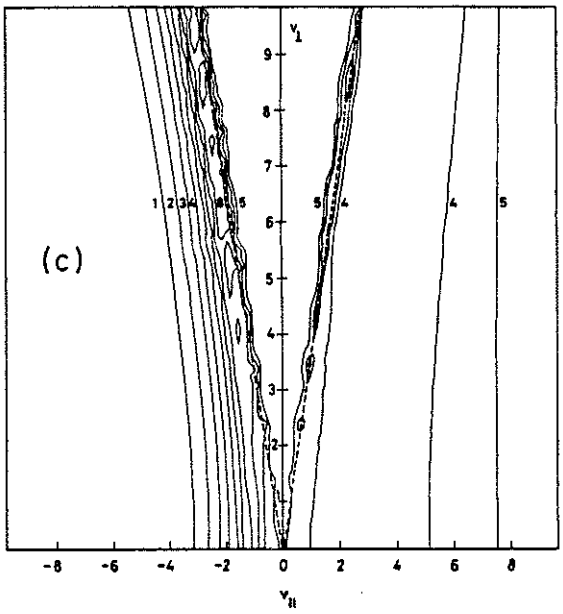

Fig.1. Contours of the magnitude of the wave diffusivity, D_0, for flux surfaces (a)-(c) of Fig.2. Each contour corresponds to a factor of two change in D_0 (with D_0 increasing with increasing contour label). The dotted line at constant pitch-angle denotes the trapped-passing boundary. The local 'hills' close to the trapped passing boundary and the lack of symmetry in the trapped region are artificial features generated by contouring a rapidly varying function defined on a relatively coarse rectangular grid.

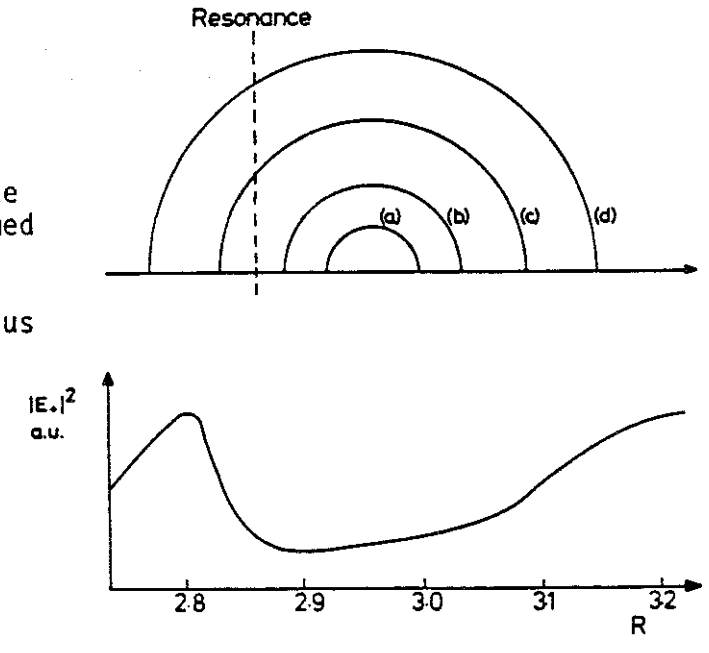

Fig.2. The upper diagram shows the cyclotron resonance position assumed throughout this work and the flux surfaces relating to Fig.1. The variation of $|E_+|^2$ with major radius is shown in the lower diagram.

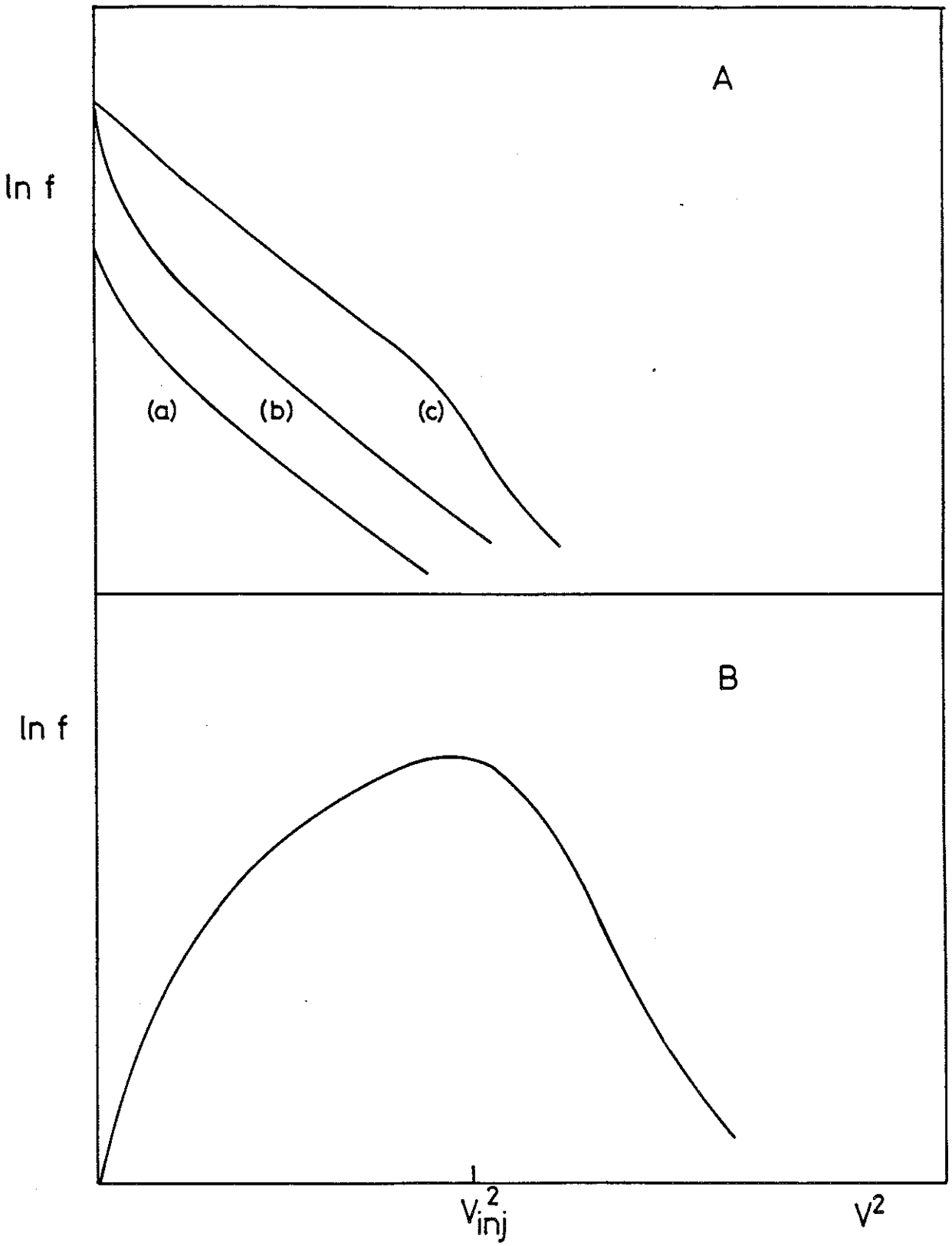

Fig.3. The two distributions (a) and (a) + (b) + (c) shown in A represent schematically the behaviour expected for, respectively, the wave and combined wave plus beam schemes. Only the distribution labelled (c), which is also shown separately in B, is used to calculate the quantities of interest. (See text for details.)

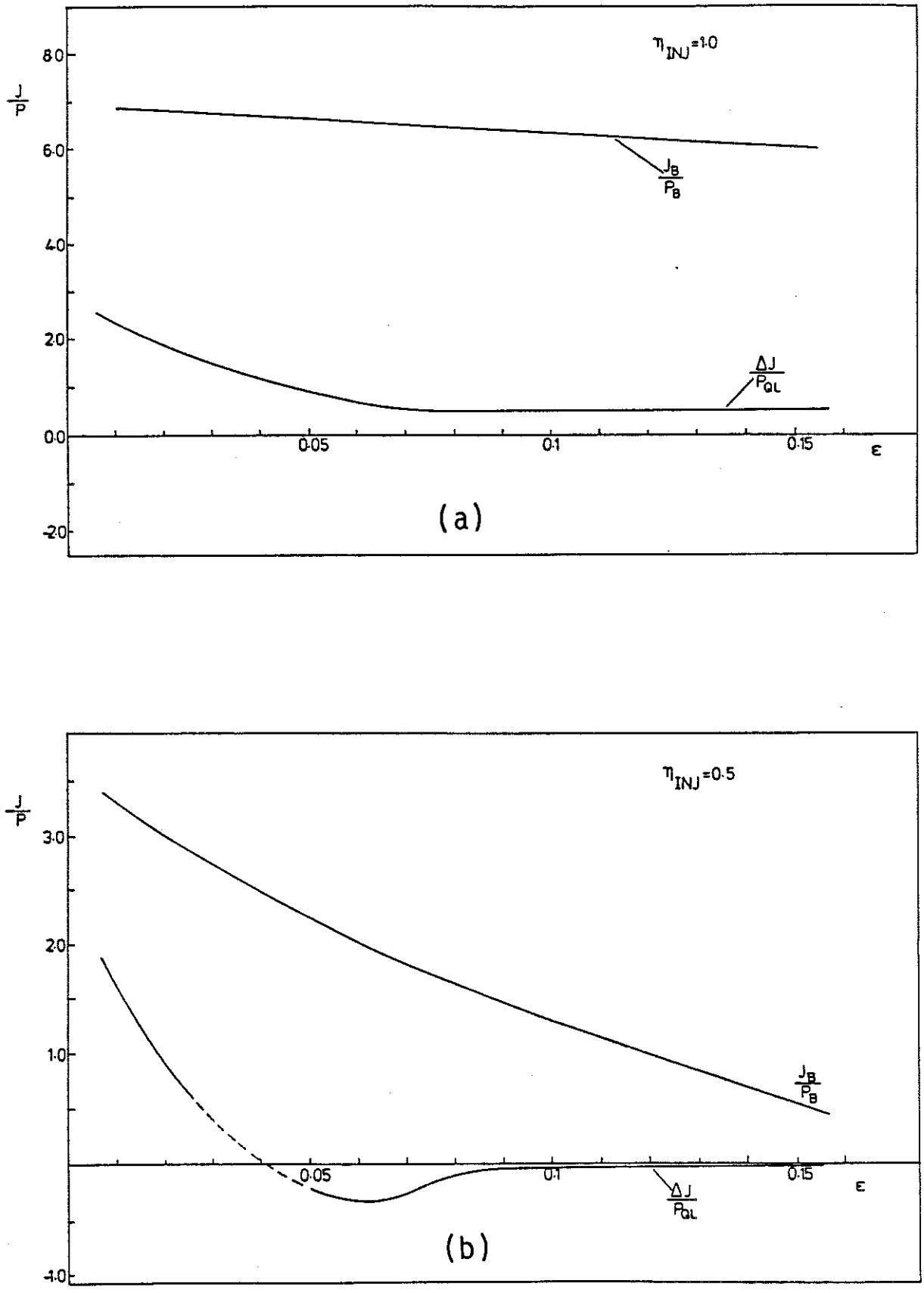

Fig.4. The current-drive efficiency for both beam and combined wave plus beam schemes for η_{INJ} = 0.5 and 1.0.

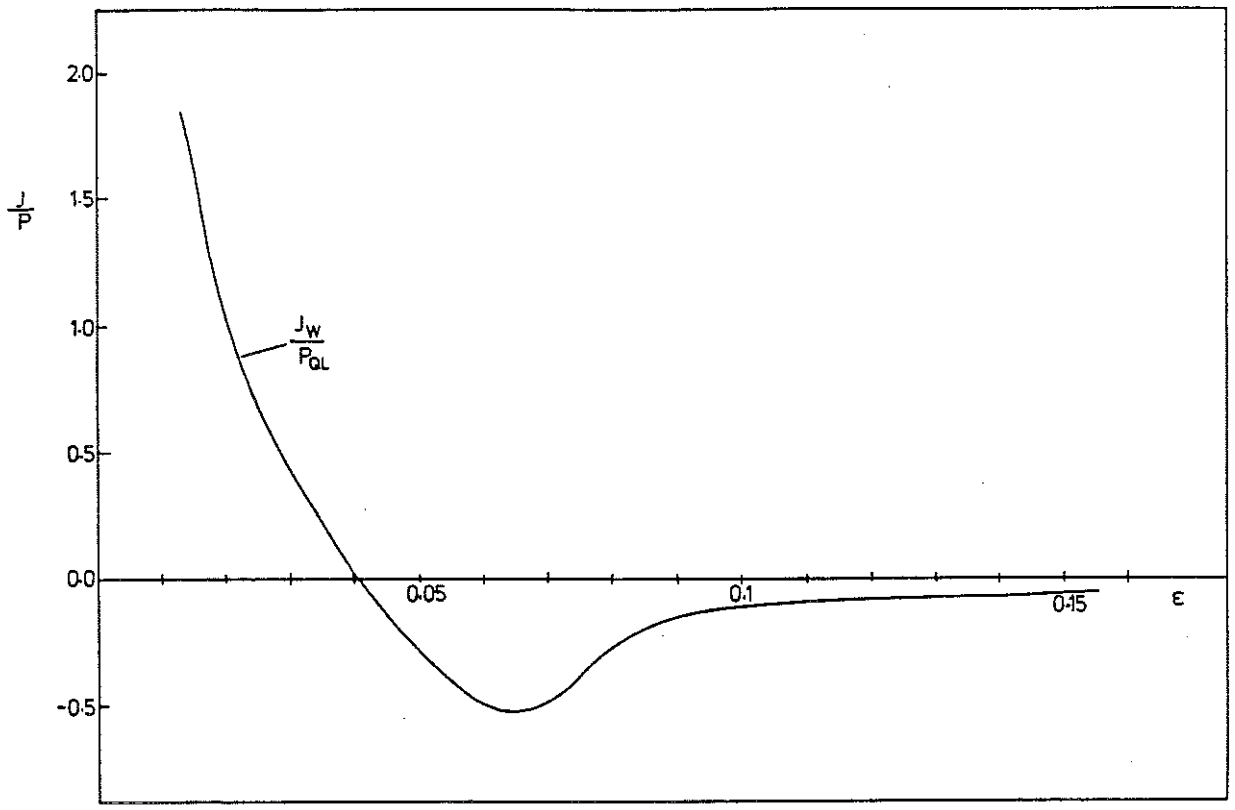

Fig.5. The current-drive efficiency for the pure wave scheme (ie, in the absence of neutral beams).

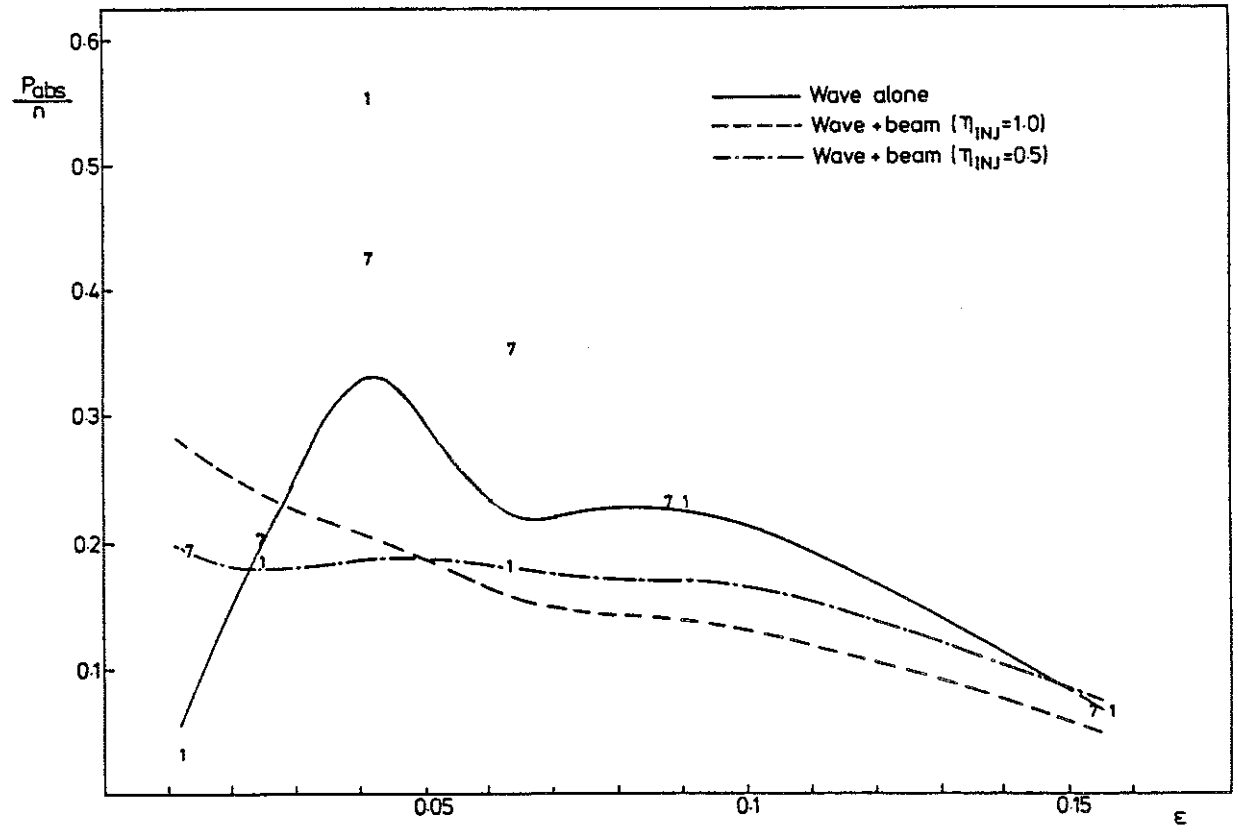

Fig.6. The power deposition per unit density as a function of minor radius for the three schemes. Also shown by the numerals 1 and 7 are the profiles obtained for absorption by Maxwellian distributions at, respectively, T_i and 7 T_i.